Reduced future North Atlantic eddy-driven jet variability in high-resolution, fully coupled global climate models

Baker, A. J. ORCID: https://orcid.org/0000-0003-2697-1350, Lockwood, J. F., Athanasiadis, P. J. and Vidale, P. L. ORCID: https://orcid.org/0000-0002-1800-8460 (2026) Reduced future North Atlantic eddy-driven jet variability in high-resolution, fully coupled global climate models. Journal of Climate. ISSN 1520-0442 doi: 10.1175/jcli-d-25-0418.1 (In Press) Available at https://centaur.reading.ac.uk/129189/

Confidential revised manuscript for submission to *Journal of Climate*

Reduced future North Atlantic eddy-driven jet variability in high-resolution, fully coupled global climate models

Alexander J. Baker[1,*], Julia F. Lockwood[2], Panos J. Athanasiadis[3], and Pier Luigi Vidale[1]

[1] National Centre for Atmospheric Science and Department of Meteorology, University of Reading, Reading, Berkshire, UK

[2] Met Office Hadley Centre, Exeter, Devon, UK

[3] Centro Euro-Mediterraneo sui Cambiamenti Climatici, Bologna, Italy

[*] Corresponding author:

Dr Alexander J. Baker
National Centre for Atmospheric Science
&
Department of Meteorology,
University of Reading
Reading, Berkshire RG6 6ES, UK
+44 (0) 118 378 7762
alexander.baker@reading.ac.uk

Early Online Release: This preliminary version has been accepted for publication in *Journal of Climate*, may be fully cited, and has been assigned DOI 10.1175/JCLI-D-25-0418.1. The final typeset copyedited article will replace the EOR at the above DOI when it is published.

Abstract

The westerly jet streams are a key component of North Atlantic climate, particularly during winter. Projections of European surface climate change depend largely on models' ability to capture jet behaviour, which requires sufficient resolution in both the atmosphere and ocean. We evaluated the impact of model resolution on the winter climatological zonal wind and on eddy-driven jet position and speed simulated under historical (1950–2014) and future (2015–2050) climate conditions in an ensemble of fully coupled global climate models, with resolution spanning ~100 to ~25 km in the atmosphere and 1 to 1/12° in the ocean. We find that increasing resolution improves the North Atlantic climatological zonal wind field at mid-to-high latitudes, but biases remain around the low-latitude, equatorward flank of the upper-level subtropical jet. By 2050, low-resolution models simulate a small equatorward shift in the mid-latitude jet, reducing the meridional separation of the subtropical and mid-latitude jets, but high-resolution models project a strengthening of the jets and a small poleward shift of the mid-latitude jet. Analysis of the large-scale meridional temperature gradient over the North Atlantic suggests that tropical amplification influences the future zonal-wind response, and there is some sensitivity of lower-level temperature gradient trends to ocean resolution. At low resolution, the eddy-driven jet shows little mean meridional shift, but increasing resolution reduces the jet's latitudinal variance. These results help clarify the role of model resolution in near-term North Atlantic climate projections and suggest further increases in atmosphere and ocean resolution may advance understanding of future jet behaviour and its downstream impacts on surface climate over Europe.

Accepted for publication in *Journal of Climate.* DOI 10.1175/JCLI-D-25-0418.1.

Significance statement

The westerly jet streams are an important part of large-scale atmospheric circulation. Over the North Atlantic, the eddy-driven component of this westerly flow steers mid-latitude storm systems towards Europe. Projections of European surface climate therefore hinge on future jet behaviour. However, projected North Atlantic circulation changes are uncertain. Increased model resolution in both the atmosphere and ocean may help reduce uncertainty. We find that projections of jet variability in latitude differ between low- and high-resolution models, and we also detect an influence of ocean resolution on trends in the large-scale meridional temperature gradients that govern mid-latitude atmospheric circulation response. These results highlight the need for high-resolution, coupled models in exploring future North Atlantic climate.

Accepted for publication in *Journal of Climate.* DOI 10.1175/JCLI-D-25-0418.1.

1. Introduction

The westerly jet streams are a key part of the large-scale atmospheric circulation over the North Atlantic. In the mid-latitudes, the lower-level, eddy-driven component of this zonal flow steers synoptic, low-pressure weather systems towards Europe (Hoskins and Hodges 2002; Woollings et al. 2018b). On the seasonal timescale, model skill in predicting jet position and the North Atlantic Oscillation are strongly related (Parker et al. 2019), highlighting the importance of the jet in modulating downstream weather. Projections of high-impact weather therefore depend largely on future jet behaviour (Harvey et al. 2023), particularly in winter, when the eddy-driven jet is most active. However, despite the importance of the jet for European surface climate, projected North Atlantic circulation changes, based on coupled climate models, remain uncertain (Blackport and Fyfe 2022; Woollings 2010). Key sources of uncertainty are an insufficient physical understanding (Shepherd 2014), significant inter-model spread (Oudar et al. 2020), and the divergence of historical model simulations from observational data (Blackport and Fyfe 2022; Smith et al. 2020).

Climate models project a strengthening and narrowing of the eddy-driven jet in response to amplified near-surface warming in the Arctic and upper-level warming in the tropics (Oudar et al. 2020; Peings et al. 2018)—two opposing influences on the jet—as well as a downstream extension in winter (Harvey et al. 2023). Based on data from phases 3–6 of the Coupled Model Intercomparison Project (CMIP), studies have described the competing effects of Arctic and tropical amplification, which act to weaken and strengthen, respectively, the westerly zonal flow. Therefore, reducing uncertainty around the magnitude of regional warming (Steiner et al. 2020) will, in principle, constrain the mid-latitude circulation response (Harvey et al. 2014; Peings et al. 2018). However, although zonal-wind biases have improved across CMIP phases 3–6 (Harvey et al. 2020; Oudar et al. 2020), uncertainties associated with the responses of individual driving mechanisms have not reduced significantly (Harvey et al. 2023). Substantial spread in simulated Arctic and tropical amplification remains evident across CMIP6 models (Oudar et al. 2020). Simulated jet responses to climate change therefore exhibit similar spatial patterns across CMIP phases (Harvey et al. 2020). Moreover, climate models fail to capture the observed jet strengthening trend (as well as the downstream precipitation trend over Europe), indicating that projections of winter atmospheric circulation (and surface climate over Europe), based on models which fail to capture the jet's forced response, may be unreliable (Blackport and Fyfe 2022).

Accepted for publication in *Journal of Climate.* DOI 10.1175/JCLI-D-25-0418.1.

Models project a poleward jet shift due to tropical warming (Barnes and Polvani 2013; Oudar et al. 2020; Simpson et al. 2014), and similar trends in the Northern Hemisphere are emerging in satellite-era reanalyses (Woollings et al. 2023). Although weak, these trends are consistent with the predominance of tropical forcing, as opposed to Arctic warming, on the jet streams. However, trends in reanalyses lie only just within the spread of CMIP6 model trends, and reanalyses show stronger trends than models despite a somewhat weaker positive temperature gradient trend compared with that simulated by models (Woollings et al. 2023). Weaker simulated trends may be due to models under-representing poleward eddy heat flux in the atmosphere, confining upper-tropospheric warming to the tropics, and insufficiently enhancing the meridional temperature gradient, inducing a weaker jet shift.

Capturing jet responses to anthropogenic climate change relies on models' ability to represent both large-scale variability and weather-scale processes. Increased horizontal resolution in climate models is therefore expected to improve the simulation of North Atlantic climate and increase confidence in climate projections (Baker et al. 2019). In fully coupled CMIP6 High-Resolution Model Intercomparison Project (HighResMIP) simulations, increasing atmosphere resolution from ~100 to ~25 km reduces sea-surface temperature (SST) and, in turn, large-scale circulation biases (Athanasiadis et al. 2022). Increased resolution also improves the representation of North Atlantic weather regime clustering, although has little impact on models' ability to reproduce observed regime frequency and persistence (Fabiano et al. 2020). Additionally, Blackport and Fyfe (2022) found little difference in simulated jet-speed trends (or trend spread) between high- and low-resolution coupled models, and found only small trend differences among simulations forced by observed SST, which suggests SST biases are unlikely to explain this disparity between models and observations. The impact of increasing resolution—in both the atmosphere and ocean—on large-scale circulation and, in turn, surface climate is therefore insufficiently well understood.

In this study, we assessed the impact of increased resolution on simulating the North Atlantic zonal wind and eddy-driven jet in historical and near-future climates. Our aims are to (i) identify differences in climate change responses that arise when horizontal resolution is increased and (ii) assess whether HighResMIP provides evidence of a response of the westerly zonal flow to ocean resolution increase. To this end, we analysed fully coupled simulations from HighResMIP over the period 1950–2050 and for boreal winter (i.e.,

Accepted for publication in *Journal of Climate.* DOI 10.1175/JCLI-D-25-0418.1.

December–February), focussing first on climatological zonal wind fields and then on the eddy-driven jet. This paper is structured as follows: model data, observational data and methods are described in section 2, results are presented in section 3, with further discussion and our conclusions summarised in section 4.

2. Data and methods

2.1 Model ensemble

This study is based on CMIP6 HighResMIP (Haarsma et al. 2016) fully coupled (Tier 2) historical and future simulations from five global climate models (Table 1): CMCC-CM2 (Cherchi et al. 2019), CNRM-CM6.1 (Voldoire et al. 2019), EC-Earth3P (Haarsma et al. 2020), HadGEM3-GC3.1 (Roberts et al. 2019; Williams et al. 2018), and MPI-ESM1.2 (Gutjahr et al. 2019). Each simulation was performed under the PRIMAVERA (PRocess-based climate sIMulation: AdVances in high-resolution modelling and European climate Risk Assessments) programme. Fully coupled historical (1950–2014) and future (2015–2050) experiments are termed *hist-1950* and *highres-future*, respectively (Haarsma et al. 2016). We analysed a single ensemble member for each model at each resolution for both *hist-1950* and *highres-future*. Additionally, we performed a separate analysis of multiple ensemble members available for HadGEM3-GC3.1 (Table S1) to help assess the extent to which multimodel results are affected by internal variability. Seddon et al. (2023) described the curation of HighResMIP data.

Under the HighResMIP experimental protocol, minimal changes in model-tuning parameters were made between low- and high-resolution integrations to ensure that analysis of resolution sensitivity is not confounded by substantial differences in model configurations between resolutions (Haarsma et al. 2016). Between low- and high-resolution configurations, no model-physics changes were made to the atmospheric components of CMCC-CM2, CNRM-CM6.1 and EC-Earth3P, and only minor adjustments were made to a single parameter in HadGEM3-GC3.1 (related to quasi-biennial oscillation period) and MPI-ESM1.2 (related to numerical stability). Shorter dynamical timesteps were used in the high-resolution integrations of all models to ensure numerical stability. The effective resolutions of the models at high resolution resolve synoptic-scale dynamics in the atmosphere (Klaver et al. 2020). For ocean models, a key difference is that the effects of mesoscale eddies are parameterised at low resolutions of ~1° but are partially resolved at high resolutions of

Accepted for publication in *Journal of Climate.* DOI 10.1175/JCLI-D-25-0418.1.

~0.25° or finer (Roberts et al. 2019). Since this study concerns mid-latitude phenomena, atmosphere resolutions are given as a model's regular mesh spacing at a latitude of 50° (Table 1). For convenience, we refer to resolutions nominally (i.e., 'low' or 'high') as well as quantitatively.

Model name	**CMCC-CM2**		**CNRM-CM6.1**		**EC-Earth3P**		**HadGEM3-GC3.1**					**MPI-ESM1.2**	
Atmosphere model	CAM4		ARPEGE6.3		IFS cyc36r4		Unified Model GA7.1					ECHAM6.3	
Atmosphere dynamical core	Grid point (finite volume)		Spectral (linear, reduced Gaussian)		Grid point (SISL)		Grid point (SISL)					Spectral (triangular; Gaussian)	
Ocean model	NEMO3.6		NEMO3.6		NEMO3.6		NEMO3.6					MPIOM1.63	
Resolution nomenclature	**HR4**	**VHR4**	**LR**	**HR**	**LR**	**HR**	**LL**	**MM**	**MH**	**HM**	**HH**	**HR**	**XR**
Atmosphere resolution at 50° [km]	100	25	142	50	71	36	135	60	60	25	25	67	34
Ocean resolution [°]	0.25	0.25	1	0.25	1	0.25	1	0.25	1/12	0.25	1/12	~0.4	~0.4

Table 1. CMIP6 HighResMIP (PRIMAVERA) model ensemble. NEMO: Nucleus for European Modelling of the Ocean. MPIOM: Max Plank Institute Ocean Model. SISL: semi-implicit, semi-Lagrangian. For most models, LR and HR denote low and high resolution, respectively, with variations for CMCC-CM2 and MPI-ESM1.2. For HadGEM3-GC3.1, LL denotes low-resolution atmosphere (135 km) and low-resolution (1°) ocean; MM denotes medium-resolution atmosphere (60 km) and medium-resolution ocean (0.25°); HM high-resolution atmosphere (25 km) and medium-resolution ocean; MH denotes medium-resolution atmosphere and high-resolution (1/12°) ocean; HH denotes high-resolution atmosphere and ocean. In this analysis, HadGEM3-GC3.1-HM is considered the high-resolution model configuration, consistent with published analyses of HighResMIP data, and the HH configuration is included for completeness. Additional ensemble members available for HadGEM3-GC3.1 are given in Table S1. Ocean model resolution is unchanged for CMCC-CM2 and MPI-ESM1.2 (TP04 / ~0.4° at the Equator). Individual digital object identifiers for each simulation are listed at primavera-h2020.eu/modelling.

Accepted for publication in *Journal of Climate*. DOI 10.1175/JCLI-D-25-0418.1.

2.2 Reanalyses

Simulations were evaluated against four global reanalyses (Table 2): the European Centre for Medium-Range Weather Forecasts' Fifth Reanalysis (ERA5; Hersbach et al. 2020); the Japanese 55-year Reanalysis (JRA55; Kobayashi et al. 2015); the National Aeronautics and Space Administration's Modern-Era Retrospective Analysis for Research and Applications version 2 (MERRA2; Molod et al. 2015); and the combined National Centers for Environmental Prediction Climate Forecast System Reanalysis and Climate Forecast System version 2 dataset (NCEP; Saha et al. 2014)—the sole fully coupled (atmosphere, ocean, land surface, and sea ice) reanalysis used herein. Reanalyses employ differing forecast model formulations, resolutions (horizontal and vertical), and data-assimilation schemes, leading to appreciable differences in the representation of large-scale phenomena (e.g., Lee et al. 2019). We therefore evaluated models against multireanalysis-mean fields.

Reanalysis	**ERA5**	**JRA55**	**MERRA2**	**NCEP**
Data assimilation	4D-Var.	4D-Var.	3D-Var., GSI, IAU	3D-Var., GSI
Resolution (grid spacing at 50°)	T639L137 (33 km)	TL319L60 (55 km)	Cubed sphere (50 km)	T382L64 (38 km)
Analysis period	1979–2018	1959–2017	1980–2018	1979–2016

Table 2. Reanalyses. Atmospheric mesh spacing at 50°N in units of km is given in parentheses. 3(4)D-Var.: 3(4)D variational data assimilation; GSI: grid-point statistical interpolation; IAU: incremental analysis update.

2.3 Meridional temperature gradients

We computed bulk meridional temperature gradients for the North Atlantic, following Lee et al. (2019). First, monthly mean temperature data were averaged over a subtropical domain (30–50°N, 10–80°W) and a subpolar domain (50–70°N, 10–80°W), both weighted by $\cos(\phi)$ to account for meridian convergence at high latitudes. The common latitudinal boundary at 50°N between these domains represents the approximate climatological annual-mean jet latitude. Second, the zonal-mean bulk meridional temperature difference across the North

Accepted for publication in *Journal of Climate.* DOI 10.1175/JCLI-D-25-0418.1.

Atlantic was computed by subtracting the subpolar area-weighted mean temperature from the subtropical area-weighted mean temperature. Finally, trends in this quantity, denoted T, were computed at multiple isobaric levels, yielding a tropospheric vertical profile of meridional temperature gradient trends for 1950–2050.

2.4 Eddy-driven jet diagnostics

The regime behaviour of the North Atlantic eddy-driven jet was examined using metrics introduced by Woollings et al. (2010) and Woollings et al. (2018b). First, daily zonal wind data at 850 hPa were zonally averaged over a North Atlantic longitudinal sector (0-60 °W) between 15 and 75 °N to capture the jet's meridional range. Second, a low-pass Lanczos filter (Duchon 1979) was applied with a 61-day window and a cut-off value of 10 days to remove wind features associated with synoptic systems. From the resulting zonal-mean westerly wind profile for each timestep, jet latitude, ϕ, was identified as the latitude at which the maximum zonal wind occurs. Grid cells where orography exceeds 750 m were masked to avoid including spurious sub-surface winds, which occur up to 850 hPa (e.g., over southern Greenland), in our analyses. An important caveat is that ϕ may be a less informative index in synoptic situations where the jet is strongly tilted or, in less common instances, where the jet is split (Perez et al. 2024).

Barnes and Polvani (2013) showed that patterns of jet variability are partly a function of jet position: as the jet shifts poleward, variability becomes less north-south and more akin to pulsing (i.e., variation in jet speed). This latitude–speed relationship is therefore a key descriptor of North Atlantic jet behaviour and included in our analysis. We examined the inverse relationship between ϕ variance and jet speed (i.e., the standard deviation of ϕ binned by jet speed). At each identified ϕ, we computed jet speed, u', as the square root of the sum of the squares of the low-pass-filtered zonal and meridional winds. Using both wind fields accounts for instances when the magnitude of jet speed is dominated by the meridional component. All data were regridded to the N96 grid of HadGEM3-GC3.1-LL to isolate resolution sensitivity from any improved sampling at higher resolution.

2.5 Significance testing

Accepted for publication in *Journal of Climate.* DOI 10.1175/JCLI-D-25-0418.1.

Significance was computed at the 99 % level using Welch's unequal variances *t*-test with respect to each individual model's internal year-to-year variability, as the HighResMIP ensemble size is insufficient to compute significance with respect to the ensemble.

3. Results

3.1 North Atlantic westerly zonal flow

We first focus on the climatological North Atlantic westerly zonal wind, quantifying multimodel-mean biases in, and the climate change response of, the vertical profile of the zonal flow during winter. The simulated zonal wind field is sensitive to model resolution. In all models except CMCC-CM2, weaker zonal winds are seen at high resolution at ~50°N, with increased winds on the equatorward and poleward flanks of the jet (Fig. S1). This indicates a larger latitudinal range of the mid-latitude jet (i.e., a broader jet) when resolution is increased, consistent with Athanasiadis et al. (2022). At low resolution, several multimodel-mean zonal wind biases (versus the multireanalysis-mean wind field) are evident (Fig. 1a). For the subtropical jet, winds are too strong on the equatorward flank. For the mid-latitude jet, winds are too strong on the equatorward flank and too weak on the poleward flank. At high resolution, mid- and high-latitude biases are significantly reduced, particularly around the jet-core latitude at low levels and the subpolar winds throughout the depth of the troposphere, but winds at high resolution remain too strong on the equatorward flank of the mid-latitude jet (Fig. 1b). Additionally, subtropical jet biases worsen somewhat, as noted by Moreno-Chamarro et al. (2022) for the annually averaged Northern Hemisphere subtropical jet. Overall, however, the climatological westerly zonal wind field across the North Atlantic is significantly better represented at high resolution. Additionally, a separate analysis of multiple ensemble members available for HadGEM3-GC3.1 (Table S1) yields similar results at high resolution (Fig. S2), supporting the multimodel results.

Accepted for publication in *Journal of Climate.* DOI 10.1175/JCLI-D-25-0418.1.

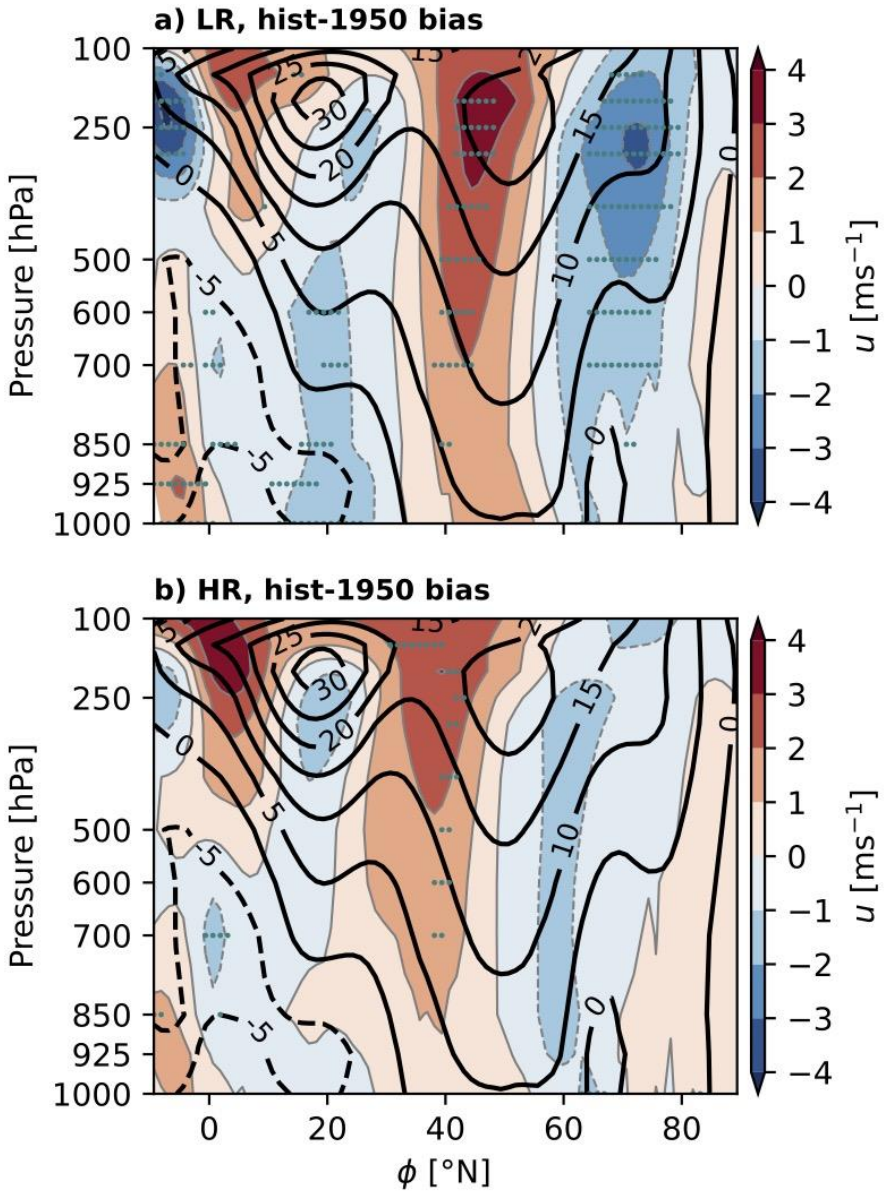

Fig. 1. Multimodel-mean climatological biases in the vertical profile of the North Atlantic westerly zonal wind averaged for December–February in (a) low- (LR) and (b) high-resolution (HR) simulations. Biases (i.e., *hist-1950* minus reanalyses; shaded contours) were computed against the multireanalysis-mean climatology (black contours). Unit is m s^{-1} and teal stippling indicates where the bias is significant at the 99 % level and where all models agree on the sign of the bias. All monthly data were regridded to the lowest-resolution model grid (HadGEM3-GC3.1-LL) to facilitate an inter-model comparison. For clarity, only selected isobaric levels are labelled on each panel's ordinate. An equivalent analysis of multiple HadGEM3-GC3.1 ensemble members (Fig. S2) yielded a similar overall pattern of biases at high resolution and at low resolution (excepting a negative bias at the equatorward flank of the subtropical jet) compared with the multimodel-mean results shown here.

Accepted for publication in *Journal of Climate.* DOI 10.1175/JCLI-D-25-0418.1.

Under climate change (to 2050), low-resolution models simulate a zonal wind decrease on the equatorward flank of the subtropical jet and poleward flank of the mid-latitude jet, with an increase in the winds between the jets (~30°N)—both at upper levels. This indicates a future reduction and shallowing of the inter-jet separation (Fig. 2). The most favourable region for baroclinic wave development lies along the subtropical jet only when the subtropical jet is sufficiently strong; a moderate-strength subtropical jet is typically associated with greater meridional separation between the subtropical and eddy-driven jets (Lee and Kim 2003). At high resolution, the weakening of mid- and upper-level westerlies at higher latitudes (poleward of ~60°N) in future is more significant (Fig. 2b). This indicates a shift towards reduced jet separation in future when resolution is increased, although this response varies across models and is clearest in CNRM-CM6.1, EC-Earth3P and HadGEM3-GC3.1 (Fig. S3). Additionally, a separate analysis of multiple HadGEM3-GC3.1 ensemble members reveals a similar ensemble-mean response for this model (Fig. S4), supporting the multimodel results. Overall, the climate change responses at low and high resolution are similar, except for the enhanced decrease in mid- and upper-level subpolar winds at high resolution, the region where a negative wind bias is significantly reduced at high resolution (Fig. 1b). Low-level responses in the mid-latitudes are uncertain. Stronger winds at high resolution are seen at ~50°N, but this response is not significant in the multimodel mean, indicating that a forced response will not emerge by 2050.

Accepted for publication in *Journal of Climate.* DOI 10.1175/JCLI-D-25-0418.1.

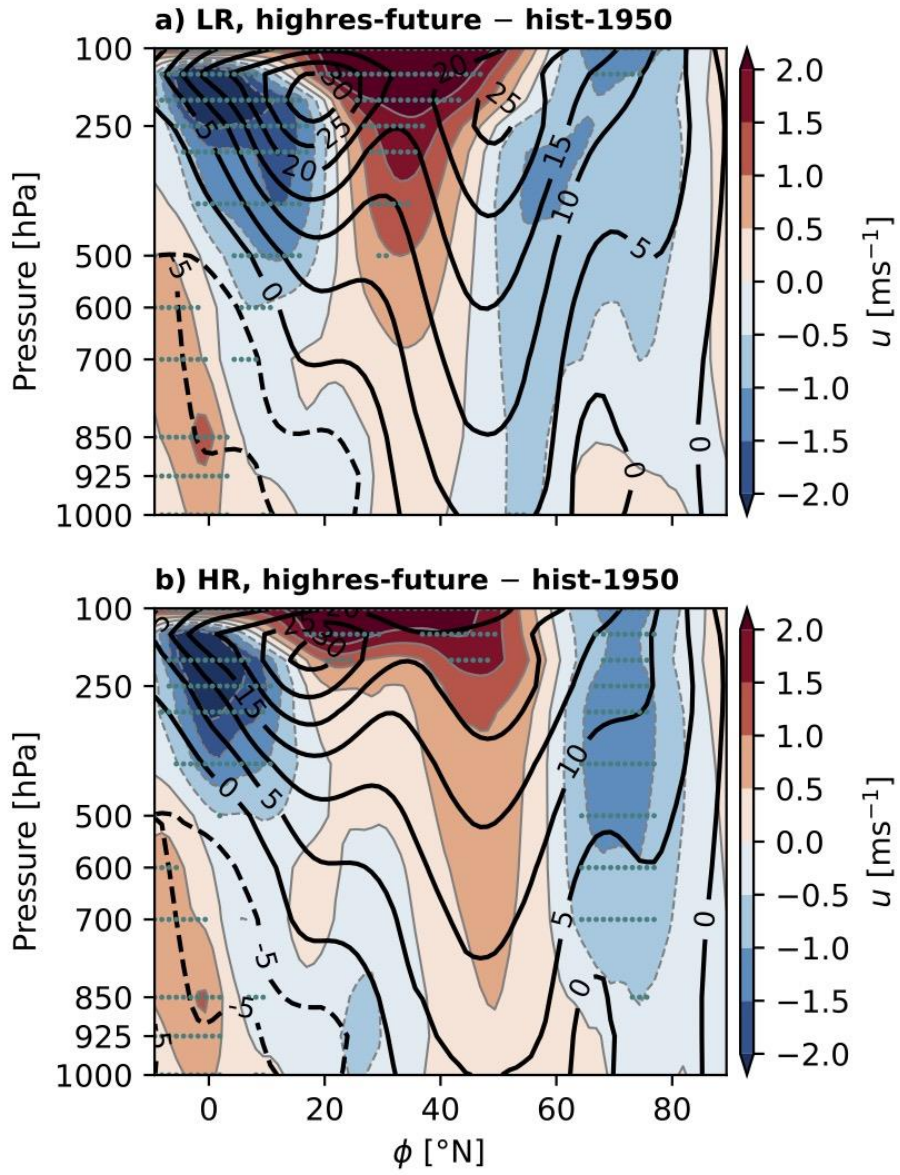

Fig. 2. Multimodel-mean climatological vertical profile of the North Atlantic westerly zonal wind averaged for December–February in (a) low- (LR) and (b) high-resolution (HR) simulations. Shown are (black contours) the multimodel-mean historical climatology (i.e., *hist-1950*) and (shaded contours) the climate change response (i.e., *highres-future* minus *hist-1950*). Differences were computed using monthly data for the 30-year periods 1950–1979 and 2020–2049. Unit is m s^{-1} and teal stippling indicates where the response is significant at the 99 % level and where all models agree on the sign of the response. All data were regridded to the lowest-resolution model grid (HadGEM3-GC3.1-LL) to facilitate an inter-model comparison. For clarity, only selected isobaric levels are labelled on each panel's ordinate. An equivalent analysis of multiple HadGEM3-GC3.1 ensemble members (Fig. S4)

Accepted for publication in *Journal of Climate.* DOI 10.1175/JCLI-D-25-0418.1.

yielded a similar overall pattern of responses compared with the multimodel-mean results shown here.

3.2 Trends in North Atlantic meridional temperature gradients

The response of the North Atlantic westerlies is sensitive to the local equator-to-pole temperature difference, *dT*/*dy* (Harvey et al. 2014). Therefore, to explain the zonal-wind responses to future forcing, we analysed trends in bulk meridional temperature gradients, computed throughout the troposphere over the simulated period (1950–2050). Negative trends exist at low levels due to Arctic amplification of warming in the lower troposphere and positive trends are seen aloft due to amplification of warming in the tropical upper troposphere (Fig. 3).

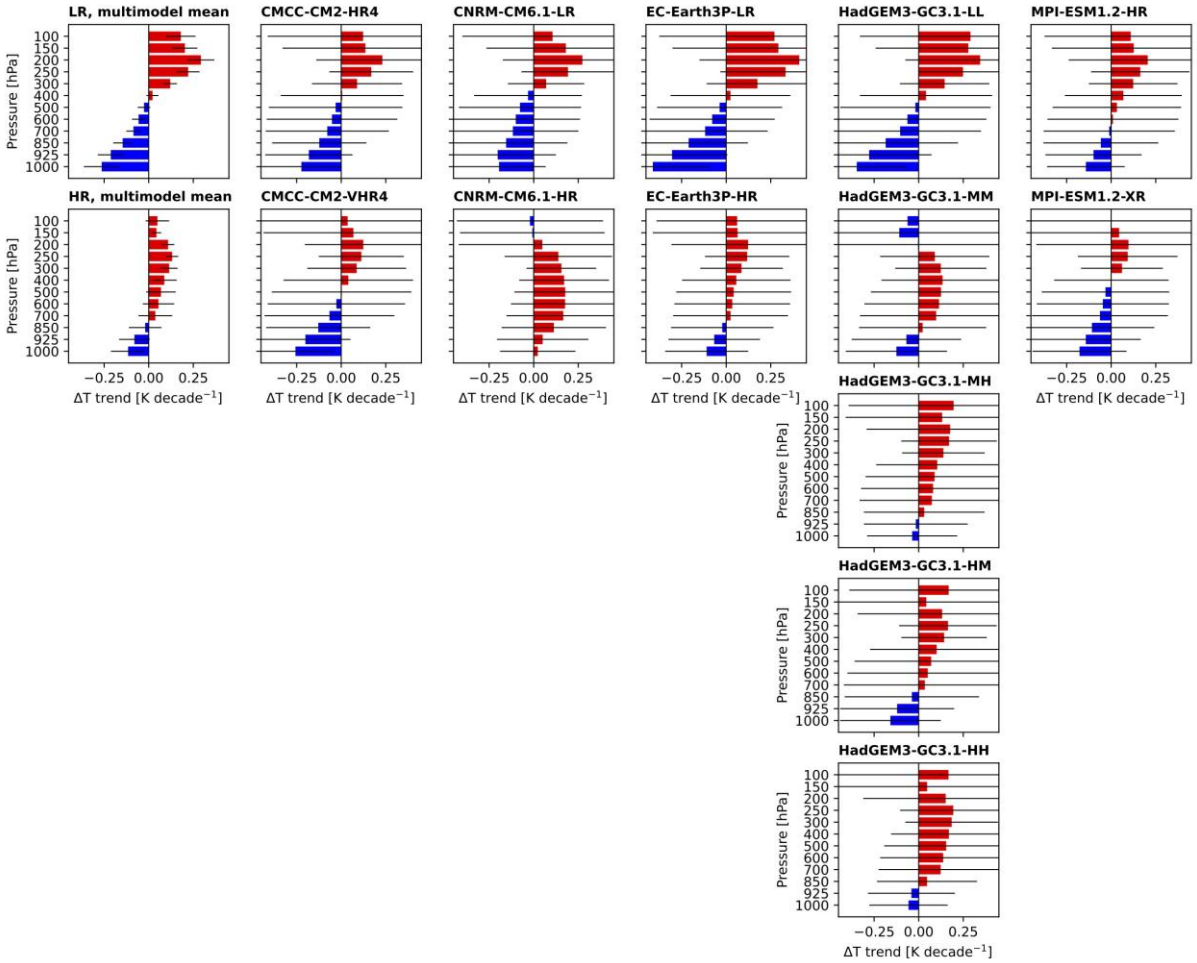

Fig. 3. Tropospheric vertical profiles of trends (1950–2050) in the winter-mean (December–February) meridional temperature difference over the North Atlantic, denoted T, in *hist-1950* and *highres-future* simulations. Multimodel-mean trends are shown (leftmost panel column) at low (LR) and high resolution (HR), with error bars denoting the standard deviation among

Accepted for publication in *Journal of Climate*. DOI 10.1175/JCLI-D-25-0418.1.

model trends. Individual model trends are separated by panel columns and available resolutions ordered low to high from top panel to bottom, with error bars denoting the 95 % confidence intervals for the linear trends. Red and blue colours denote positive and negative trends, respectively.

At low resolution, the vertical profile of multimodel-mean trends in HighResMIP is generally consistent with those derived from reanalysis datasets (Lee et al. 2019), albeit computed over a longer time frame here (Fig. 3). Several differences between low- and high-resolution simulations are apparent. At low resolution, the transition from negative to positive trends occurs between 400 and 500 hPa, consistent with reanalyses. However, this transition occurs at a lower level (between 850 and 700 hPa) at high resolution (Fig. 3). Additionally, individual high-resolution models exhibit their strongest positive trends at different levels in the mid and upper troposphere (Fig. 3). The magnitudes of negative and positive trends in the lower and upper troposphere, respectively, are weaker in the high-resolution multimodel mean, and this is also generally true of individual models, particularly EC-Earth3P and HadGEM3-GC3.1. These results may to some extent be influenced by the lack of model retuning of the global energy balance at high resolution, an aspect of the HighResMIP protocol (Haarsma et al. 2016).

There is an indication that ocean resolution influences bulk meridional temperature gradients. CMCC-CM2 and MPI-ESM1.2 show little change in low-level negative trends between atmosphere resolutions (Fig. 3), and these are models where ocean resolution is unchanged. For HadGEM3-GC3.1, simulations performed with different ocean resolutions (ranging from 1 to 1/12°) allow insight into the impact of partially resolving ocean eddies. HadGEM3-GC3.1 shows a clear decrease in the magnitudes of low-level negative trends with increasing ocean resolution (Fig. 3). Comparing simulations with ocean resolutions of 0.25° (MM) and 1/12° (MH) for the same atmosphere resolution (60 km) shows less pronounced low-level negative trends with the higher-resolution ocean. Conversely, simulations with atmosphere resolutions of 60 (MH) and 25 km (HH) for the same ocean resolution (1/12°) exhibit highly similar vertical profiles. These results highlight the possible influence of ocean resolution on the bulk meridional temperature gradients which modulate mid-latitude circulation. Potentially, this reflects higher poleward eddy heat transport at high ocean resolution (Roberts et al. 2019) acting to reduce the low-level gradients via air–sea interactions (Gulev et al. 2013). However, an initial analysis of surface turbulent heat fluxes (not shown) did not

Accepted for publication in *Journal of Climate.* DOI 10.1175/JCLI-D-25-0418.1.

reveal similar sensitivity to ocean resolution. An important caveat here is that a larger multimodel ensemble, including multiple ocean resolutions, is required to investigate this.

In these coupled simulations, future zonal-wind changes at each isobaric level with respect to changes at the surface (i.e., the vertical wind shear) are in near-exact thermal wind balance with the changes in meridional temperature gradient (Fig. S5). Blackport and Fyfe (2022) and Woollings et al. (2023) reported that dT/dy in the upper troposphere is stronger in models than observational data, yet concurrent changes in the upper-tropospheric zonal wind are smaller than expected from this temperature gradient. This implies that simulated zonal wind trends are not in accordance with thermal wind balance. However, we find that thermal wind balance holds when the integral of dT/dy (over 1000 hPa to a given isobaric level) is taken instead of a single level.

Lee et al. (2019) showed that the compensating influences of the lower- and upper-level meridional temperature gradient trends result in no discernible historical trend in upper-level mid-latitude zonal wind speed. Here, given thermal wind balance holds, we attempt to relate differences between the low- and high-resolution tropospheric trend profiles with differences between the low- and high-resolution zonal-wind responses (Fig. 2). These trends in meridional temperature gradients are generally consistent with the simulated future responses of the North Atlantic zonal wind field. Stronger winds aloft at both low and high resolution (Fig. 2) may be explained by the positive trends in meridional temperature gradients at upper levels. At low resolution, strengthened future westerly winds occur above ~500 hPa, but strengthened mid-latitude winds are present at lower levels (above ~850 hPa) at high resolution—both consistent with the approximate levels at which the transitions between negative and positive temperature trends occur. HighResMIP models therefore provide further evidence that tropical amplification is potentially a stronger actor in determining the future zonal-wind response. A caveat to this interpretation, however, is the relatively small ensemble size of HighResMIP.

3.3 North Atlantic eddy-driven jet

In this section, we analyse the eddy-driven jet using a jet-latitude index, which describes three regimes: northern (~53–60°N), central (~45–50°N), and southern (~35–40°N). This apparent trimodality of the eddy-driven jet is captured by HighResMIP models (Fig. 4a), an aspect not adequately simulated by a majority of CMIP5 models (Iqbal et al. 2018) nor by

Accepted for publication in *Journal of Climate.* DOI 10.1175/JCLI-D-25-0418.1.

several CMIP6 models over the central and eastern North Atlantic (Dorrington et al. 2022; Oudar et al. 2020). The most frequent central jet-latitude regime is better simulated at high resolution (Fig. 4a), confirming a complementary analysis of HighResMIP simulations (Athanasiadis et al. 2022) and atmosphere-only, single-model results (Baker et al. 2019). The northern regime is less prominent in the HighResMIP multimodel mean compared with reanalyses (Fig. 4a), which is also seen in CMIP6 models (Oudar et al. 2020). Furthermore, the distribution of jet latitude variance as a function of jet speed (percentile), described by a characteristic negative curve, is also better captured at high resolution (Fig. 4c). At low resolution, simulated variance is too low compared with reanalyses, although greater inter-reanalysis and inter-model spread are evident at lower speed percentiles.

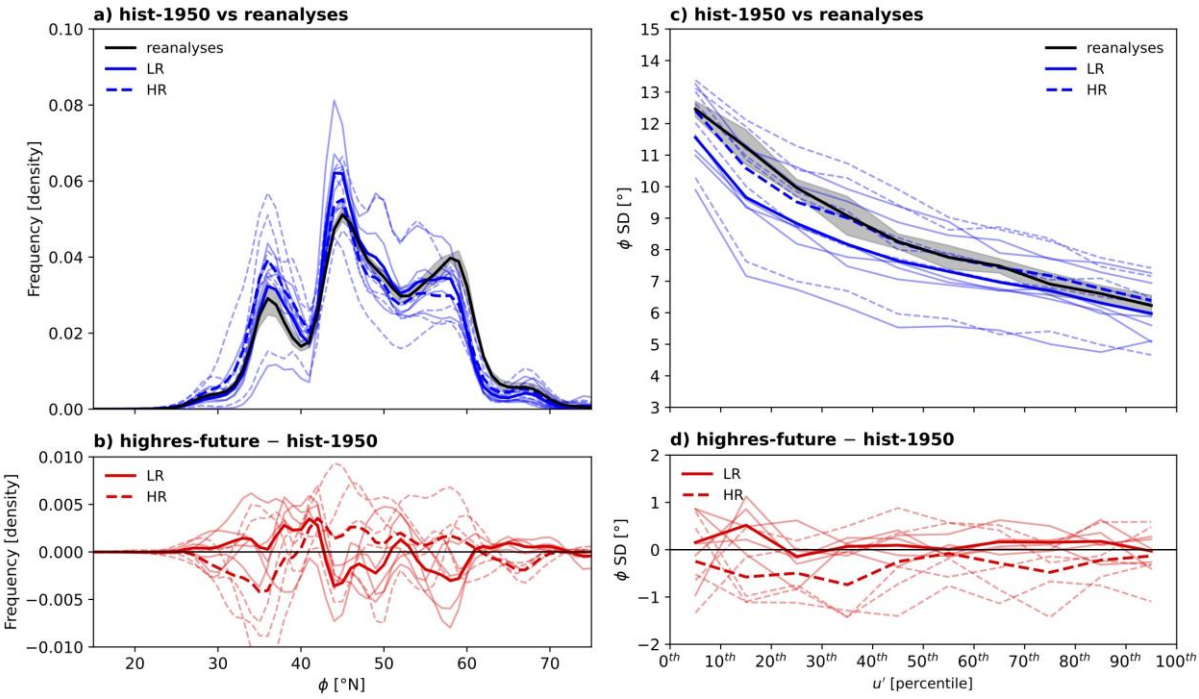

Fig. 4. (a) Frequency distribution of December–February eddy-driven jet latitude, ϕ, computed using low-pass-filtered daily data following Woollings et al. (2010) for reanalyses and *hist-1950* simulations (*highres-future* distributions are shown in Fig. S6). (b) Response of ϕ in *highres-future* simulations. Unit in (a) and (b) is normalised frequency density. (c) Standard deviation of ϕ as a function of jet speed, *u'*, (given as percentiles, with a bin width of 10 %), computed from low-pass-filtered daily zonal and meridional wind fields following Woollings et al. (2018b). (d) Response of ϕ variance in *highres-future* simulations. Unit in (c) and (d) is degrees. Grey shading in (a) and (c) indicates the standard deviation of reanalyses. Shown in all panels are multimodel-mean (bold lines) and individual model (thin lines)

Accepted for publication in *Journal of Climate.* DOI 10.1175/JCLI-D-25-0418.1.

curves for low- (LR; solid) and high-resolution (HR; dashed) simulations. An equivalent analysis of multiple HadGEM3-GC3.1 ensemble members is shown in Fig. S7.

Under climate change, the multimodel-mean response of jet latitude at low resolution is a frequency decrease in the central and northern regimes and an increase in the southern regime—in other words, an equatorward shift (Fig. 4b). At high resolution, however, responses differ: a frequency increase in the central and northern regimes and a decrease in the southern regime—in other words, a poleward shift (Fig. 4b). Strictly, these are shifts in the frequencies of each jet regime, rather than in the absolute latitudes at which regimes occur (Fig. S6). Additionally, reduced meridional variability is projected at high resolution (Fig. 4c), indicating a narrowing of the jet that is consistent with the mean westerly flow (Fig. 2). A separate analysis of the available HadGEM3-GC3.1 ensemble members (Table S1) reveals a poleward shift across resolutions for this model, and this shift is stronger at high resolution (Fig. S7a), consistent with Baker et al. (2019) and broadly corroborating multimodel results. The climate change response of variance in jet latitude is also sensitive to resolution. At low resolution, the response of jet latitude variance is close to zero at all speed percentiles (Fig. 4d). At high resolution, however, a decrease in variance is simulated at nearly all speed percentiles (Fig. 4d), indicating a more persistent jet. For this diagnostic, high-resolution simulations are potentially more trustworthy because the historical latitude–speed relationship is ostensibly closer to reanalyses at ~25 km resolution. A separate analysis of the HadGEM3-GC3.1 ensemble also shows little change of jet latitude variance at low resolution but reduced variance across speed percentiles at high resolution (Fig. S7b), substantiating the multimodel result. This is consistent with a meridional narrowing of the westerly flow (Peings et al. 2018) and reduced winter blocking (Gao et al. 2025; Woollings et al. 2018a), although differs from a recent analysis of lower-resolution CMIP6 models (Dorrington et al. 2022). These results are somewhat inconsistent with an analysis of large-scale waviness in HighResMIP (Yamamoto and Martineau 2024), which showed a significant reduction in atmospheric waviness at low resolution but a less clear response at high resolution, although their model ensemble differs from that of this study (Table 1). Additionally, historical HighResMIP simulations show limited improvement with increased resolution in capturing persistent episodes of European blocking (Schiemann et al. 2020), indicating that some sensitivity to the metric used to characterise large-scale variability exists.

Accepted for publication in *Journal of Climate.* DOI 10.1175/JCLI-D-25-0418.1.

To examine eddy-driven jet behaviour in more detail, we analysed bivariate distributions of jet latitude and speed. The multireanalysis-mean bivariate distribution shows that the central jet regime is associated with higher jet speeds compared with the northern and southern regimes (Fig. 5a), and the southern regime is associated particularly with low speeds. Reanalyses show little variation (Fig. S8, upper row). To evaluate simulated bivariate distributions, multimodel-mean biases (Fig. 5b–c) and individual model biases (Fig. S8, middle and lower rows) were computed. At low resolution, there is a clear positive bias for the central jet regime at ~45°N, and negative biases are seen for both the southern and northern jet regimes (Fig. 5b). At high resolution, the central jet regime bias is reduced (Fig. 5c), which is important because this is both the most frequent regime and the regime associated with the strongest steering flow for low-pressure weather systems impacting Europe (Baker et al. 2019; Harvey et al. 2023; Woollings et al. 2018b). However, at high resolution, the negative northern regime bias persists, and a positive bias emerges between 30–40°N, where high-resolution models simulate high-speed southern jet instances that are not present in reanalyses. This low-latitude bias in the multimodel mean is predominantly due to CNRM-CM6.1 and MPI-ESM1.2 (Fig. S8). Additionally, simulated historical distributions show an equatorward shift in jet latitude when resolution is increased (Fig. 5d), with less frequent central and northern jet occurrences, particularly at higher speed percentiles, and more frequent southern jet occurrences (Fig. 5d), consistent with both the resolution sensitivity of the mean zonal wind (Fig. 1) and with a recent complementary analysis of the North Atlantic mid-latitude storm track (Lockwood et al. 2025). Although the multimodel-mean climatological variance in jet latitude as a function of jet speed is better represented at high resolution (Fig. 4c), diverse individual model biases are found in HighResMIP (Fig. S8). The occurrence of each jet-latitude regime at a particular range in jet speed, as apparent in reanalyses, is not better captured when resolution is increased from ~100 to ~25 km in the mid-latitudes.

Accepted for publication in *Journal of Climate.* DOI 10.1175/JCLI-D-25-0418.1.

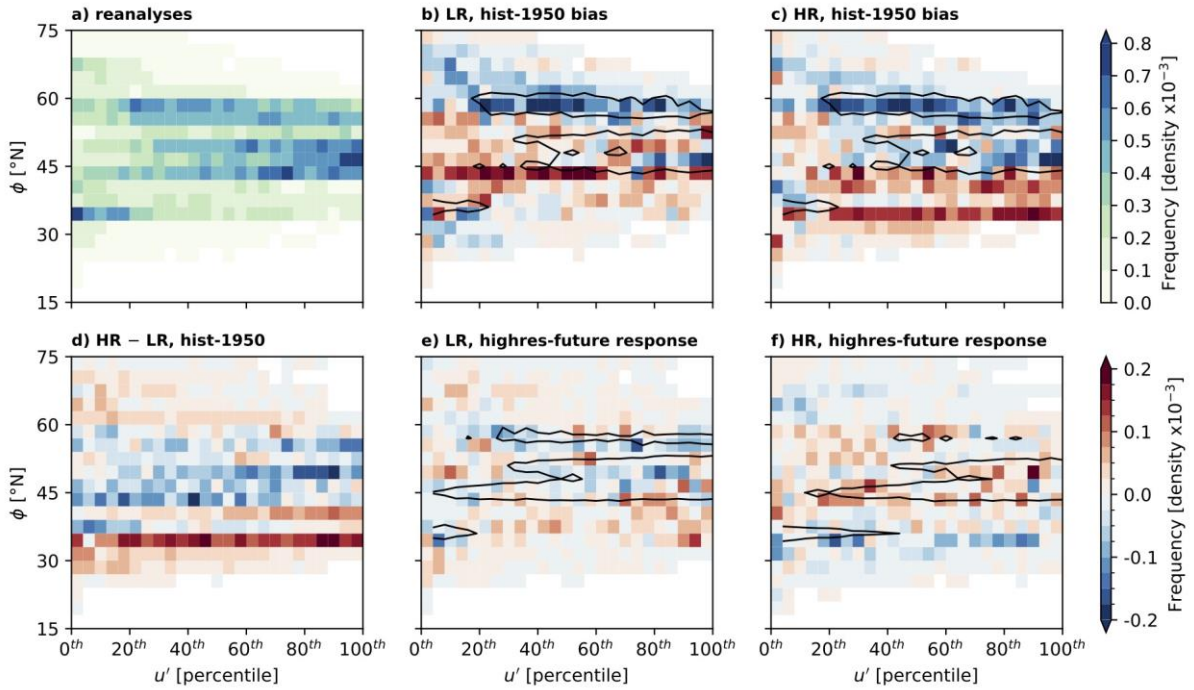

Fig. 5. Bivariate distributions of December–February eddy-driven jet latitude, ϕ, and jet speed, u', (percentiles) in (a) reanalyses, and multimodel-mean biases in these quantities in (b) low- (LR) and (c) high-resolution (HR) *hist-1950* simulations; (c) sensitivity to resolution (i.e., HR minus LR); and the multimodel-mean climate change response (i.e., *highres-future* minus *hist-1950*) at (d) LR and (e) HR. Zonal and meridional wind fields were low-pass-filtered as in Fig. 4 and the unit is normalised frequency density ($\times 10^{-3}$). Overlain black contour (at 0.4×10^{-3}) indicates the multireanalysis-mean field in (b) and (c) and the historical multimodel-mean field in (e) and (f). Reanalyses are shown individually in Fig. S8.

Under climate change, changes in latitude–speed distributions are small. At low resolution, a small equatorward shift is projected, but the overall pattern is equivocal (Fig. 5e). At high-resolution, projected increases in frequency across northern and central jet regimes are clearest, with decreases across the southern regime and smaller decreases in the lowest and highest latitudes (Fig. 5f), again resulting in a narrowed jet (and a relative poleward shift), consistent with Fig. 4d. Additionally, at high resolution, the eddy-driven jet's response to climate change may be influenced by the equatorward-shifted historical mean state (Fig. 5d). The two models for which ocean resolution is unchanged (CMCC-CM2 and MPI-ESM1.2) exhibit little difference between low- and high-resolution responses (Fig. S9), again indicating that dynamical coupling with a higher-resolution ocean may influence the circulation response.

Accepted for publication in *Journal of Climate.* DOI 10.1175/JCLI-D-25-0418.1.

4. Summary and discussion

4.1 Main results

In this study, we assessed the impact of model resolution on the winter climatological zonal wind and eddy-driven jet position and speed, simulated under historical (1950–2014) and future (2015–2050) climate conditions in an ensemble of fully coupled global climate models at resolutions ranging from ~100 to ~25 km in the atmosphere and 1 to 1/12° in the ocean. Increasing resolution significantly improves the representation of the mid-latitude jet and its eddy-driven component, and responses to climate change differ between low- and high-resolution simulations. The main findings of our work are:

- Increasing resolution significantly improves (versus reanalyses) the North Atlantic climatological zonal wind field at mid and high latitudes, but biases remain around the low-latitude, equatorward flank of the upper-level subtropical jet (Fig. 1).
- By 2050, low-resolution models simulate an equatorward shift in the mid-latitude jet, reducing the upper-level meridional separation of the subtropical and mid-latitude jets, but high-resolution models project a strengthening of the jets and a small poleward shift of the mid-latitude jet (Fig. 2).
- Trends in the large-scale meridional temperature gradient over the North Atlantic suggests that tropical amplification influences the future zonal-wind response, and there is an indication of sensitivity of lower-level temperature gradient trends to ocean resolution (Fig. 3).
- At low resolution, the eddy-driven jet shows little mean meridional shift under climate change. At high resolution, however, climate change reduces the jet's latitudinal variance (Fig. 4 and Fig. 5).

4.2. Discussion and outlook

In HighResMIP simulations, future zonal-wind changes at a given isobaric level with respect to changes at the surface (i.e., the vertical wind shear) are in thermal wind balance with the changes in meridional temperature gradient. To explain models' zonal-wind responses to future forcing, we analysed trends in meridional temperature gradients. These trends were found to be generally consistent with the simulated future responses of the North Atlantic zonal wind field. Strengthened future westerly winds aloft (Fig. 2) may be explained by

Accepted for publication in *Journal of Climate.* DOI 10.1175/JCLI-D-25-0418.1.

positive trends in meridional temperature gradients at upper levels. Stronger westerlies occur above ~500 hPa at low resolution above ~850 hPa at high resolution, consistent with the approximate levels at which the transitions between negative and positive temperature gradient trends occur (Fig. 3). In HighResMIP, tropical amplification appears a stronger actor in determining the future zonal-wind response, consistent with recent analyses (Oudar et al. 2020; Woollings et al. 2023). CMIP6 models overestimate warming of the tropical middle (Mitchell et al. 2020) and upper (Blackport and Fyfe 2022) troposphere. These biases are potentially due to the representation of convection in low-resolution CMIP6 models, which tend to overestimate the amount of upper-tropospheric warming for a given level of lower-tropospheric warming (Keil et al. 2021; Mitchell et al. 2020). This is due to low entrainment rates warming the upper troposphere by allowing convection and latent heating further aloft. Further increases in atmosphere resolution to reduce reliance on parameterised convection may resolve this (Blackport and Fyfe 2022).

We also analysed the eddy-driven component of the westerly flow, focussing on jet position and on variance in jet position as a function of jet speed. HighResMIP models capture the trimodality of the jet-latitude index, which CMIP5 and several CMIP6 models do not, and both the overall distribution of jet latitude and the variance of jet latitude as a function of jet speed are better simulated at high resolution (Fig. 4). This indicates that resolution is a key component of capturing eddy-driven jet behaviour in models. However, the occurrence of each jet-latitude regime at a typical range in jet speed, which is seen in reanalyses, is not well captured when resolution is increased from ~100 to 25 km in the mid-latitudes. Under climate change, the eddy-driven jet shifts equatorward at low resolution but narrows and shifts poleward at high resolution. Increased ocean resolution may influence the high-resolution near-future response, but a key caveat to these results is that the ensemble size considered here is relatively small.

To help increase confidence in atmospheric circulation projections, future work should focus on expanding the ensemble size, by conducting ensemble simulations for multiple models, and further increasing model resolution in both the atmosphere and ocean. In HighResMIP, the use of an eddy-permitting ocean model in a fully coupled framework increases blocking frequency (Athanasiadis et al. 2022), and SST biases are improved significantly in models where ocean resolution is increased (or physics improved) alongside increased atmosphere resolution (Moreno-Chamarro et al. 2022). Finer resolution may improve model biases

Accepted for publication in *Journal of Climate.* DOI 10.1175/JCLI-D-25-0418.1.

further, as eddy forcing is too weak in HighResMIP models (Dorrington et al. 2022), leading to under-persistent regime behaviour (Fabiano et al. 2020). This study provides evidence that jet latitude regime-persistence increases at ~25 km, but, together with existing studies of the same simulations (Blackport and Fyfe 2022; Dorrington et al. 2022; Fabiano et al. 2020; Moreno-Chamarro et al. 2022; Schiemann et al. 2020), indicates that the contribution of eddy forcing to North Atlantic climate variability remains insufficiently captured. Here, we see evidence of influence of ocean resolution on trends in low-level meridional temperature gradients, which do not change in coupled models where ocean resolution is constant. With an eddy-permitting ocean resolution, low-level temperature gradients are reduced, an effect that may be enhanced by the higher eddy activity in response to warming seen in recent eddy-rich ocean modelling (Beech et al. 2022; Li et al. 2024).

Models may also underestimate the magnitude of multidecadal and centennial internal variability (Marcheggiani et al. 2023; Smith et al. 2020). Centennial-length simulations extending beyond 2050 are needed to address two outstanding concerns. First, this study indicates that climate change signals in eddy-driven jet latitude and speed may not emerge by 2050. The projected atmospheric circulation response to Arctic sea-ice loss is also weak (Smith et al. 2022) and much uncertainty remains around the impact of Arctic amplification on mid-latitude weather (Cohen et al. 2014). Second, proxy evidence points to high internal variability, enveloping recent observed jet shifts, which makes extracting anthropogenically forced changes challenging (Osman et al. 2021). Longer, higher-resolution simulations with fully coupled models, such as those proposed by Roberts et al. (2025), may help address the uncertainty around changes in North Atlantic atmospheric circulation and surface climate over the twenty-first century.

Accepted for publication in *Journal of Climate.* DOI 10.1175/JCLI-D-25-0418.1.

Data and code availability

Reanalysis data are available from cds.climate.copernicus.eu, rda.ucar.edu or disc.gsfc.nasa.gov. Model data are available from Earth System Grid Foundation nodes (esgf.llnl.gov). Data analysis and visualisation code is available from the corresponding author upon request.

Acknowledgements

The authors are grateful to the modelling teams that produced the PRIMAVERA simulations and to J. Seddon for data curation. All authors received financial support from the PRIMAVERA project (European Commission Horizon2020 grant agreement 641727) with data access supported by IS-ENES3 (grant agreement 824084) via the JASMIN facility (jasmin.ac.uk), which is operated by the Science and Technology Facilities Council on behalf of the Natural Environment Research Council. AJB received additional support from a Natural Environment Research Council national capability programme, the North Atlantic Climate System: Integrated Study (grant agreements NE/N018001/1, NE/N018044/1, NE/N018028/1, and NE/N018052/1).

Author contributions

AJB and PLV conceived the study. AJB performed data analysis, figure preparation, and wrote the manuscript. JFL performed the analysis presented in Fig. S5. All authors approved the final manuscript draft.

Competing interests

The authors declare no competing interests.

References

Athanasiadis, P. J., F. Ogawa, N.-E. Omrani, N. Keenlyside, R. Schiemann, A. J. Baker, P. L. Vidale, A. Bellucci, P. Ruggieri, R. Haarsma, M. Roberts, C. Roberts, L. Novak, and S. Gualdi, 2022: Mitigating Climate Biases in the Midlatitude North Atlantic by Increasing Model Resolution: SST Gradients and Their Relation to Blocking and the Jet. *Journal of Climate*, **35,** 3379–3400.

Baker, A. J., R. Schiemann, K. I. Hodges, M.-E. Demory, M. S. Mizielinski, M. J. Roberts, L. C. Shaffrey, J. Strachan, and P. L. Vidale, 2019: Enhanced Climate Change Response of Wintertime North Atlantic Circulation, Cyclonic Activity, and Precipitation in a 25-km-Resolution Global Atmospheric Model. *Journal of Climate*, **32,** 7763–7781.

Barnes, E. A., and L. Polvani, 2013: Response of the Midlatitude Jets, and of Their Variability, to Increased Greenhouse Gases in the CMIP5 Models. *Journal of Climate*, **26,** 7117–7135.

Beech, N., T. Rackow, T. Semmler, S. Danilov, Q. Wang, and T. Jung, 2022: Long-term evolution of ocean eddy activity in a warming world. *Nature Climate Change*, **12,** 910–917.

Blackport, R., and J. C. Fyfe, 2022: Climate models fail to capture strengthening wintertime North Atlantic jet and impacts on Europe. *Science Advances*, **8,** eabn3112.

Cherchi, A., P. G. Fogli, T. Lovato, D. Peano, D. Iovino, S. Gualdi, S. Masina, E. Scoccimarro, S. Materia, A. Bellucci, and A. Navarra, 2019: Global Mean Climate and Main Patterns of Variability in the CMCC-CM2 Coupled Model. *Journal of Advances in Modeling Earth Systems*, **11,** 185–209.

Cohen, J., J. A. Screen, J. C. Furtado, M. Barlow, D. Whittleston, D. Coumou, J. Francis, K. Dethloff, D. Entekhabi, J. Overland, and J. Jones, 2014: Recent Arctic amplification and extreme mid-latitude weather. *Nature Geoscience*, **7,** 627–637.

Dorrington, J., K. Strommen, and F. Fabiano, 2022: Quantifying climate model representation of the wintertime Euro-Atlantic circulation using geopotential-jet regimes. *Weather and Climate Dynamics*, **3,** 505–533.

Duchon, C. E., 1979: Lanczos Filtering in One and Two Dimensions. *Journal of Applied Meteorology*, **18,** 1016–1022.

Accepted for publication in *Journal of Climate.* DOI 10.1175/JCLI-D-25-0418.1.

Fabiano, F., H. M. Christensen, K. Strommen, P. Athanasiadis, A. Baker, R. Schiemann, and S. Corti, 2020: Euro-Atlantic weather Regimes in the PRIMAVERA coupled climate simulations: impact of resolution and mean state biases on model performance. *Climate Dynamics*, **54,** 5031–5048.

Gao, Y., X. Guo, J. Lu, T. Woolings, D. Chen, X. Guo, W. Kou, S. Zhang, L. R. Leung, R. Schiemann, C. H. O'Reilly, C. Guo, J. Li, H. Gao, and L. Wu, 2025: Enhanced Simulation of Atmospheric Blocking in a High-Resolution Earth System Model: Projected Changes and Implications for Extreme Weather Events. *Journal of Geophysical Research: Atmospheres*, **130,** e2024JD042045.

Gulev, S. K., M. Latif, N. Keenlyside, W. Park, and K. P. Koltermann, 2013: North Atlantic Ocean control on surface heat flux on multidecadal timescales. *Nature*, **499,** 464–467.

Gutjahr, O., D. Putrasahan, K. Lohmann, J. H. Jungclaus, J. S. von Storch, N. Brüggemann, H. Haak, and A. Stössel, 2019: Max Planck Institute Earth System Model (MPI-ESM1.2) for the High-Resolution Model Intercomparison Project (HighResMIP). *Geoscientific Model Development*, **12,** 3241–3281.

Haarsma, R., M. Acosta, R. Bakhshi, P. A. Bretonnière, L. P. Caron, M. Castrillo, S. Corti, P. Davini, E. Exarchou, F. Fabiano, U. Fladrich, R. Fuentes Franco, J. García-Serrano, J. von Hardenberg, T. Koenigk, X. Levine, V. L. Meccia, T. van Noije, G. van den Oord, F. M. Palmeiro, M. Rodrigo, Y. Ruprich-Robert, P. Le Sager, E. Tourigny, S. Wang, M. van Weele, and K. Wyser, 2020: HighResMIP versions of EC-Earth: EC-Earth3P and EC-Earth3P-HR – description, model computational performance and basic validation. *Geoscientific Model Development*, **13,** 3507–3527.

Haarsma, R. J., M. J. Roberts, P. L. Vidale, C. A. Senior, A. Bellucci, Q. Bao, P. Chang, S. Corti, N. S. Fučkar, V. Guemas, J. von Hardenberg, W. Hazeleger, C. Kodama, T. Koenigk, L. R. Leung, J. Lu, J. J. Luo, J. Mao, M. S. Mizielinski, R. Mizuta, P. Nobre, M. Satoh, E. Scoccimarro, T. Semmler, J. Small, and J. S. von Storch, 2016: High Resolution Model Intercomparison Project (HighResMIP v1.0) for CMIP6. *Geoscientific Model Development*, **9,** 4185–4208.

Accepted for publication in *Journal of Climate.* DOI 10.1175/JCLI-D-25-0418.1.

Harvey, B., E. Hawkins, and R. Sutton, 2023: Storylines for future changes of the North Atlantic jet and associated impacts on the UK. *International Journal of Climatology*, **43,** 4424–4441.

Harvey, B. J., L. C. Shaffrey, and T. J. Woollings, 2014: Equator-to-pole temperature differences and the extra-tropical storm track responses of the CMIP5 climate models. *Climate Dynamics*, **43,** 1171–1182.

Harvey, B. J., P. Cook, L. C. Shaffrey, and R. Schiemann, 2020: The Response of the Northern Hemisphere Storm Tracks and Jet Streams to Climate Change in the CMIP3, CMIP5, and CMIP6 Climate Models. *Journal of Geophysical Research: Atmospheres*, **125,** e2020JD032701.

Hersbach, H., B. Bell, P. Berrisford, S. Hirahara, A. Horányi, J. Muñoz-Sabater, J. Nicolas, C. Peubey, R. Radu, D. Schepers, A. Simmons, C. Soci, S. Abdalla, X. Abellan, G. Balsamo, P. Bechtold, G. Biavati, J. Bidlot, M. Bonavita, G. De Chiara, P. Dahlgren, D. Dee, M. Diamantakis, R. Dragani, J. Flemming, R. Forbes, M. Fuentes, A. Geer, L. Haimberger, S. Healy, R. J. Hogan, E. Hólm, M. Janisková, S. Keeley, P. Laloyaux, P. Lopez, C. Lupu, G. Radnoti, P. de Rosnay, I. Rozum, F. Vamborg, S. Villaume, and J.-N. Thépaut, 2020: The ERA5 global reanalysis. *Quarterly Journal of the Royal Meteorological Society*, **146,** 1999–2049.

Hoskins, B. J., and K. I. Hodges, 2002: New Perspectives on the Northern Hemisphere Winter Storm Tracks. *Journal of the Atmospheric Sciences*, **59,** 1041–1061.

Iqbal, W., W.-N. Leung, and A. Hannachi, 2018: Analysis of the variability of the North Atlantic eddy-driven jet stream in CMIP5. *Climate Dynamics*, **51,** 235–247.

Keil, P., H. Schmidt, B. Stevens, and J. Bao, 2021: Variations of Tropical Lapse Rates in Climate Models and Their Implications for Upper-Tropospheric Warming. *Journal of Climate*, **34,** 9747–9761.

Klaver, R., R. Haarsma, P. L. Vidale, and W. Hazeleger, 2020: Effective resolution in high resolution global atmospheric models for climate studies. *Atmospheric Science Letters*, **21,** e952.

Accepted for publication in *Journal of Climate.* DOI 10.1175/JCLI-D-25-0418.1.

Kobayashi, S., Y. Ota, Y. Harada, A. Ebita, M. Moriya, H. Onoda, K. Onogi, H. Kamahori, C. Kobayashi, H. Endo, K. Miyaoka, and K. Takahashi, 2015: The JRA-55 Reanalysis: General Specifications and Basic Characteristics. *Journal of the Meteorological Society of Japan. Ser. II*, **93,** 5–48.

Lee, S., and H.-k. Kim, 2003: The Dynamical Relationship between Subtropical and Eddy-Driven Jets. *Journal of the Atmospheric Sciences*, **60,** 1490–1503.

Lee, S. H., P. D. Williams, and T. H. A. Frame, 2019: Increased shear in the North Atlantic upper-level jet stream over the past four decades. *Nature*, **572,** 639–642.

Li, X., Q. Wang, S. Danilov, N. Koldunov, C. Liu, V. Müller, D. Sidorenko, and T. Jung, 2024: Eddy activity in the Arctic Ocean projected to surge in a warming world. *Nature Climate Change*, **14,** 156–162.

Lockwood, J. F., P. J. Athanasiadis, A. J. Baker, K. Hodges, M. D. K. Priestley, M. Roberts, A. A. Scaife, P.-L. Vidale, and G. Zappa, 2025: The Effect of Increasing Model Resolution on the Northern Hemisphere Winter Midlatitude Storm Track: An Equatorward Shift due to Contraction of the Hadley Cell. *Journal of Climate*, **38,** 4539–4551.

Marcheggiani, A., J. Robson, P.-A. Monerie, T. J. Bracegirdle, and D. Smith, 2023: Decadal Predictability of the North Atlantic Eddy-Driven Jet in Winter. *Geophysical Research Letters*, **50,** e2022GL102071.

Mitchell, D. M., Y. T. Eunice Lo, W. J. M. Seviour, L. Haimberger, and L. M. Polvani, 2020: The vertical profile of recent tropical temperature trends: Persistent model biases in the context of internal variability. *Environmental Research Letters*, **15,** 1040b1044.

Molod, A., L. Takacs, M. Suarez, and J. Bacmeister, 2015: Development of the GEOS-5 atmospheric general circulation model: evolution from MERRA to MERRA2. *Geoscientific Model Development*, **8,** 1339–1356.

Moreno-Chamarro, E., L. P. Caron, S. Loosveldt Tomas, J. Vegas-Regidor, O. Gutjahr, M. P. Moine, D. Putrasahan, C. D. Roberts, M. J. Roberts, R. Senan, L. Terray, E. Tourigny, and P. L. Vidale, 2022: Impact of increased resolution on long-standing biases in HighResMIP-PRIMAVERA climate models. *Geoscientific Model Development*, **15,** 269–289.

Accepted for publication in *Journal of Climate.* DOI 10.1175/JCLI-D-25-0418.1.

Osman, M. B., S. Coats, S. B. Das, J. R. McConnell, and N. Chellman, 2021: North Atlantic jet stream projections in the context of the past 1,250 years. *Proceedings of the National Academy of Sciences*, **118,** e2104105118.

Oudar, T., J. Cattiaux, and H. Douville, 2020: Drivers of the Northern Extratropical Eddy-Driven Jet Change in CMIP5 and CMIP6 Models. *Geophysical Research Letters*, **47,** e2019GL086695.

Parker, T., T. Woollings, A. Weisheimer, C. O'Reilly, L. Baker, and L. Shaffrey, 2019: Seasonal Predictability of the Winter North Atlantic Oscillation From a Jet Stream Perspective. *Geophysical Research Letters*, **46,** 10159–10167.

Peings, Y., J. Cattiaux, S. J. Vavrus, and G. Magnusdottir, 2018: Projected squeezing of the wintertime North-Atlantic jet. *Environmental Research Letters*, **13,** 074016.

Perez, J., A. C. Maycock, S. D. Griffiths, S. C. Hardiman, and C. M. McKenna, 2024: A new characterisation of the North Atlantic eddy-driven jet using two-dimensional moment analysis. *Weather and Climate Dynamics*, **5,** 1061–1078.

Roberts, M. J., A. Baker, E. W. Blockley, D. Calvert, A. Coward, H. T. Hewitt, L. C. Jackson, T. Kuhlbrodt, P. Mathiot, C. D. Roberts, R. Schiemann, J. Seddon, B. Vannière, and P. L. Vidale, 2019: Description of the resolution hierarchy of the global coupled HadGEM3-GC3.1 model as used in CMIP6 HighResMIP experiments. *Geoscientific Model Development*, **12,** 4999–5028.

Roberts, M. J., K. A. Reed, Q. Bao, J. J. Barsugli, S. J. Camargo, L. P. Caron, P. Chang, C. T. Chen, H. M. Christensen, G. Danabasoglu, I. Frenger, N. S. Fučkar, S. ul Hasson, H. T. Hewitt, H. Huang, D. Kim, C. Kodama, M. Lai, L. Y. R. Leung, R. Mizuta, P. Nobre, P. Ortega, D. Paquin, C. D. Roberts, E. Scoccimarro, J. Seddon, A. M. Treguier, C. Y. Tu, P. A. Ullrich, P. L. Vidale, M. F. Wehner, C. M. Zarzycki, B. Zhang, W. Zhang, and M. Zhao, 2025: High-Resolution Model Intercomparison Project phase 2 (HighResMIP2) towards CMIP7. *Geoscientific Model Development*, **18,** 1307–1332.

Saha, S., S. Moorthi, X. Wu, J. Wang, S. Nadiga, P. Tripp, D. Behringer, Y.-T. Hou, H.-y. Chuang, M. Iredell, M. Ek, J. Meng, R. Yang, M. P. Mendez, H. v. d. Dool, Q. Zhang, W.

Wang, M. Chen, and E. Becker, 2014: The NCEP Climate Forecast System Version 2. *Journal of Climate*, **27,** 2185–2208.

Schiemann, R., P. Athanasiadis, D. Barriopedro, F. Doblas-Reyes, K. Lohmann, M. J. Roberts, D. V. Sein, C. D. Roberts, L. Terray, and P. L. Vidale, 2020: Northern Hemisphere blocking simulation in current climate models: evaluating progress from the Climate Model Intercomparison Project Phase 5 to 6 and sensitivity to resolution. *Weather and Climate Dynamics*, **1,** 277–292.

Seddon, J., A. Stephens, M. S. Mizielinski, P. L. Vidale, and M. J. Roberts, 2023: Technology to aid the analysis of large-volume multi-institute climate model output at a central analysis facility (PRIMAVERA Data Management Tool V2.10). *Geoscientific Model Development*, **16,** 6689–6700.

Shepherd, T. G., 2014: Atmospheric circulation as a source of uncertainty in climate change projections. *Nature Geoscience*, **7,** 703–708.

Simpson, I. R., T. A. Shaw, and R. Seager, 2014: A Diagnosis of the Seasonally and Longitudinally Varying Midlatitude Circulation Response to Global Warming. *Journal of the Atmospheric Sciences*, **71,** 2489–2515.

Smith, D. M., R. Eade, M. B. Andrews, H. Ayres, A. Clark, S. Chripko, C. Deser, N. J. Dunstone, J. García-Serrano, G. Gastineau, L. S. Graff, S. C. Hardiman, B. He, L. Hermanson, T. Jung, J. Knight, X. Levine, G. Magnusdottir, E. Manzini, D. Matei, M. Mori, R. Msadek, P. Ortega, Y. Peings, A. A. Scaife, J. A. Screen, M. Seabrook, T. Semmler, M. Sigmond, J. Streffing, L. Sun, and A. Walsh, 2022: Robust but weak winter atmospheric circulation response to future Arctic sea ice loss. *Nature Communications*, **13,** 727.

Smith, D. M., A. A. Scaife, R. Eade, P. Athanasiadis, A. Bellucci, I. Bethke, R. Bilbao, L. F. Borchert, L. P. Caron, F. Counillon, G. Danabasoglu, T. Delworth, F. J. Doblas-Reyes, N. J. Dunstone, V. Estella-Perez, S. Flavoni, L. Hermanson, N. Keenlyside, V. Kharin, M. Kimoto, W. J. Merryfield, J. Mignot, T. Mochizuki, K. Modali, P. A. Monerie, W. A. Müller, D. Nicolí, P. Ortega, K. Pankatz, H. Pohlmann, J. Robson, P. Ruggieri, R. Sospedra-Alfonso, D. Swingedouw, Y. Wang, S. Wild, S. Yeager, X. Yang, and L. Zhang, 2020: North Atlantic climate far more predictable than models imply. *Nature*, **583,** 796–800.

Accepted for publication in *Journal of Climate.* DOI 10.1175/JCLI-D-25-0418.1.

Steiner, A. K., F. Ladstädter, W. J. Randel, A. C. Maycock, Q. Fu, C. Claud, H. Gleisner, L. Haimberger, S. P. Ho, P. Keckhut, T. Leblanc, C. Mears, L. M. Polvani, B. D. Santer, T. Schmidt, V. Sofieva, R. Wing, and C. Z. Zou, 2020: Observed Temperature Changes in the Troposphere and Stratosphere from 1979 to 2018. *Journal of Climate*, **33,** 8165–8194.

Voldoire, A., D. Saint-Martin, S. Sénési, B. Decharme, A. Alias, M. Chevallier, J. Colin, J. F. Guérémy, M. Michou, M. P. Moine, P. Nabat, R. Roehrig, D. Salas y Mélia, R. Séférian, S. Valcke, I. Beau, S. Belamari, S. Berthet, C. Cassou, J. Cattiaux, J. Deshayes, H. Douville, C. Ethé, L. Franchistéguy, O. Geoffroy, C. Lévy, G. Madec, Y. Meurdesoif, R. Msadek, A. Ribes, E. Sanchez-Gomez, L. Terray, and R. Waldman, 2019: Evaluation of CMIP6 DECK Experiments With CNRM-CM6-1. *Journal of Advances in Modeling Earth Systems*, **11,** 2177–2213.

Williams, K. D., D. Copsey, E. W. Blockley, A. Bodas-Salcedo, D. Calvert, R. Comer, P. Davis, T. Graham, H. T. Hewitt, R. Hill, P. Hyder, S. Ineson, T. C. Johns, A. B. Keen, R. W. Lee, A. Megann, S. F. Milton, J. G. L. Rae, M. J. Roberts, A. A. Scaife, R. Schiemann, D. Storkey, L. Thorpe, I. G. Watterson, D. N. Walters, A. West, R. A. Wood, T. Woollings, and P. K. Xavier, 2018: The Met Office Global Coupled Model 3.0 and 3.1 (GC3.0 and GC3.1) Configurations. *Journal of Advances in Modeling Earth Systems*, **10,** 357–380.

Woollings, T., 2010: Dynamical influences on European climate: an uncertain future. *Philosophical Transactions of the Royal Society A: Mathematical, Physical and Engineering Sciences*, **368,** 3733–3756.

Woollings, T., A. Hannachi, and B. Hoskins, 2010: Variability of the North Atlantic eddy-driven jet stream. *Quarterly Journal of the Royal Meteorological Society*, **136,** 856–868.

Woollings, T., M. Drouard, C. H. O'Reilly, D. M. H. Sexton, and C. McSweeney, 2023: Trends in the atmospheric jet streams are emerging in observations and could be linked to tropical warming. *Communications Earth & Environment*, **4,** 125.

Woollings, T., D. Barriopedro, J. Methven, S.-W. Son, O. Martius, B. Harvey, J. Sillmann, A. R. Lupo, and S. Seneviratne, 2018a: Blocking and its Response to Climate Change. *Current Climate Change Reports*, **4,** 287–300.

Accepted for publication in *Journal of Climate.* DOI 10.1175/JCLI-D-25-0418.1.

Woollings, T., E. Barnes, B. Hoskins, Y.-O. Kwon, R. W. Lee, C. Li, E. Madonna, M. McGraw, T. Parker, R. Rodrigues, C. Spensberger, and K. Williams, 2018b: Daily to Decadal Modulation of Jet Variability. *Journal of Climate*, **31,** 1297–1314.

Yamamoto, A., and P. Martineau, 2024: On the Driving Factors of the Future Changes in the Wintertime Northern-Hemisphere Atmospheric Waviness. *Geophysical Research Letters*, **51,** e2024GL108793.

Accepted for publication in *Journal of Climate.* DOI 10.1175/JCLI-D-25-0418.1.